Video Article

Folding and Characterization of a Bio-responsive Robot from DNA Origami

Yaniv Amir[1], Almogit Abu-Horowitz[1], Ido Bachelet[1]

[1]Faculty of Life Sciences and the Institute for Nanotechnology & Advanced Materials, Bar-Ilan University

Correspondence to: Ido Bachelet at ido.bachelet@biu.ac.il

Abstract

The DNA nanorobot is a hollow hexagonal nanometric device, designed to open in response to specific stimuli and present cargo sequestered inside. Both stimuli and cargo can be tailored according to specific needs. Here we describe the DNA nanorobot fabrication protocol, with the use of the DNA origami technique. The procedure initiates by mixing short single-strand DNA staples into a stock mixture which is then added to a long, circular, single-strand DNA scaffold in presence of a folding buffer. A standard thermo cycler is programmed to gradually lower the mixing reaction temperature to facilitate the staples-to-scaffold annealing, which is the guiding force behind the folding of the nanorobot. Once the 60 hr folding reaction is complete, excess staples are discarded using a centrifugal filter, followed by visualization via agarose-gel electrophoresis (AGE). Finally, successful fabrication of the nanorobot is verified by transmission electron microscopy (TEM), with the use of uranyl-formate as negative stain.

Video Link

The video component of this article can be found at https://www.jove.com/video/51272/

Introduction

The uses for nucleic acids nanotechnology are astounding. The tractability of the Watson-Crick base pairing as well as the ease and relative low-cost of large-scale synthesis of custom-made oligos[2] has generated an explosion of applications[3] and research in the field of DNA nanotechnology. Structural DNA nanotechnology, based on the immobile Seeman junction[4,5] as a fundamental building block makes use of DNA as a self-assembling elementary unit for the construction of arbitrary shapes[6-8].

The recent development of the scaffolded DNA origami[9] technique allows for the construction of complex 2D/3D nano-architectures[10-12] with sub-nanometer precision and is an efficient route for building new functional objects with increasing complexity and astonishing diversity. The construction process is based upon a long scaffold single stranded DNA, usually derived from a viral genome, which can be folded through the hybridization of hundreds of short single strand DNA oligos termed staples. The high structural resolution obtained by this technique is the direct result of the natural dimensions of the DNA double helix, while the reproducibility of fabrication is the result of tailoring the short single-strand staple sequences to facilitate the maximum hydrogen-bonding complementarity achievable. With the use of a slow temperature annealing ramp the designed lowest-energy, thermodynamically preferred nanostructure is reached in high yields and fidelity. The easy implementation of junction design rules in a computer code enabled the development of CAD tools, such as caDNAno[13], that extremely simplify the task of designing large, complex structures containing hundreds of connected junctions.

Previously we described the design of a DNA nanorobot with the aid of the caDNAno tool[14,15]. Here we depict the fabrication and visualization, via transmission electron microscopy (TEM), of the nanorobot, a 3D hollow hexagonal nanodevice, with dimensions of 35 x 35 x 50 nm^3, designed to undergo a major conformational change in response to a predetermined stimuli and present specific cargo, such as proteins or nucleic acid oligos, sequestered inside. While 12 loading stations are available inside the hollow chassis, the actual number of bound cargo differs with cargo size. Cargo molecules range from small DNA molecules to enzymes, antibodies and 5-10 nm gold nanoparticles. Cargo can either be uniform or heterogeneous, such that each nanorobot contains a mixture of different molecules. Sensing is achieved via two double helical locking gates design to sense proteins, nucleic acids or other chemicals, based either on aptasensor[16,17] or DNA strand displacement[18] technologies. Recent developments in aptamer selection protocols[19-21] enable the design of nanorobots responding to an ever increasing range of molecules and cell types.

Earlier work showed a nanorobot carrying a specific antibody, which upon binding to its antigen can relay either an inhibitory or a prolific signal to the inside of specific cell types in a mixed cell population[15]. An exciting feature of these nanodevices is their ability to perform even more complex tasks and logic control with the introduction of different nanorobot subtypes in a single population. Recently we demonstrated specific subtypes of nanorobots performing as either positive or negative regulators, controlling an effector population containing an active cargo molecule[22].

The protocol presented here describes the fabrication, purification and imaging of a nanorobot gated with aptamer sensor sequences which bind selectively to PDGF to facilitate the opening of the nanorobot[15,22]. The fabrication process described is similar to the nanorobot fabrication process initially depicted by Douglas et al.[15] with changes aimed at reducing overall process duration, while increasing the yield and purification rates.

Protocol

1. Preparation of Staples Pool Mixture

1. Order lyophilized DNA nanorobot staples on 96-well plates as listed in **Table 1** (see **Materials**) and normalize to 10 nmol. For a detailed description of the design and architecture of the DNA nanorobot see Ben-Ishay et al.[14] and Douglas et al.[15]).
2. Reconstitute each staple well with DNase/RNase-free ultrapure to a concentration of 100 µM. For staples normalized to 10 nmol, reconstitute with 100 µl of ultrapure water.
3. Pool together 20 µl of each staple using a multichannel pipettor and a sterile 55 ml solution basin.
   Note: Since the nanorobot shape is comprised of 254 staple strands (including Core, Edges, Handles and Guides sequences, **Table 1**), the concentration of each of the staples in the staples pool is 394 nM. Removing staples from the staple pool, or adding some at different volumes, may reduce the yield considerably, or otherwise result in unfolded aggregates.

2. Preparation of Fabrication Reaction Mixture

1. For a standard reaction mixture use 40 µl of M13mp18 viral genome circular single strand DNA, corresponding to 4 pmol of scaffold DNA (100 nM stock solution, see **Materials**). Final concentration of scaffold in the fabrication mixture is 20 nM, final volume 200 µl.
   1. Adjust the amount of scaffold DNA according to specific needs; however, keep the final concentration of scaffold DNA in the reaction mixture at a constant 20 nM.

2. Add staples to reach a scaffold to staples ratio of 1 to 10, respectively. For a 20 nM scaffold DNA concentration, each of the 254 staples' final concentration is 200 nM. For a 200 µl final reaction volume add 102 µl of the staples pool mixture (section 1.2).
   1. Add specific Gate sequences separately to the folding reaction mixture at this time. These oligos are ordered separately and require HPLC purification. Ensure that Gate oligos are present in a 1:10 scaffold to Gate sequence ratio, i.e. 200 nM of each oligo for a 20 nM scaffold concentration. For a 200 µl folding reaction volume, add 0.4 µl for each of the four Gate oligo at a 100 µM stock concentration.

3. Add 10x TAE stock buffer to reach a final concentration of 1x TAE (40 mM Tris-Acetate, 1 mM EDTA). For a 200 µl folding reaction volume, add 20 µl of 10x TAE.
4. Add 1 M $MgCl_2$ to a final concentration of 10 mM. For a 200 µl folding reaction volume, add 2 µl of 1 M $MgCl_2$.
5. Add 36 µl of DNase/RNase free ultrapure water to a reach a final volume of 200 µl.
6. Vortex and aliquot 100 µl samples into PCR vials.
   Note: Consult thermal cycler specification regarding the maximum reaction volumes to be used. Reducing the volume to meet these limits will not reduce the yields obtained. Reaction volumes above the maximum specified will jeopardize the yields.

3. Temperature Annealing Ramp of Fabrication Reaction

1. Program thermal cycler as followed:
   1. Ramp 85 °C to 60 °C at a rate of 5 min/°C.
   2. Ramp 60 °C to 4 °C at a rate of 75 min/°C.
   3. Hold at 4 °C indefinitely.

2. After fabrication has ended store samples at -20 °C.

4. Removal of Excess Staples

1. Add 100 µl of folding reaction mixture to a 0.5 ml centrifugal filter with a MWCO of 100 kDa. Save a 10 µl sample of nanorobots pre-purification for later analysis.
2. Centrifuge for 10 min at 9,600 x g.
3. Add 400 µl of folding buffer (1x TAE, 10 mM $MgCl_2$).
4. Repeat steps 4.2 and 4.3 twice more.
5. Centrifuge for 5 min at 9,600 x g.
6. Recover the concentrate by placing the filter upside down in a clean microcentrifuge tube and spin for 1 min at 9,600 x g. Final volumes may vary depending on the initial volume of fabrication reaction mixture that was put into the filter. Typically a 25-60 µl final volume of concentrated nanorobot sample is obtained.
7. Measure concentration of DNA in the samples via spectrophotometer at 260 nm. Use molecular weight of 5.3 µg/pmol when calculating molar concentrations of nanorobot samples.
   Note: The molar extinction coefficient for dsDNA, 50 µg/OD$_{260,}$ is sufficient for most applications. 48 µg/OD$_{260}$ takes into account the poly thymine ssDNA stretches at the Edges staples.

5. Agarose Gel Electrophoresis Analysis of Folded Nanorobots

1. Preparation of 0.5x TBE (45 mM Tris-Borate, 1 mM EDTA), 2% agarose gel supplemented with 10 mM $MgCl_2$ (adapted from Ernesto Castro et al.[21]):
    1. Prepare 0.5x TBE buffer by diluting 6.25 ml of 10x TBE stock buffer in 118.75 ml of ddH_2O.
    2. Dissolve 2.5 g of agarose in 125 ml of 0.5x TBE buffer.
    3. Boil in microwave until the agarose is completely dissolved.
    4. Add 1.25 ml of 1 M $MgCl_2$ to final concentration of 10 mM.
    5. Add 7 µl of 10 mg/ml ethidium bromide.
    6. Wait for solution to slightly cool and fill the gel tray before the agarose gel solidifies. Install desired comb immediately.
    7. Prepare 1 L 0.5x TBE running buffer by adding 50 ml of 10x TBE stock buffer and 10 ml of 1 M $MgCl_2$ to 940 ml of ddH_2O.
    8. Once gel is solid add running buffer to the electrophoresis device and put device in an ice bath.

2. Load 1 µg total DNA of the nanorobots pre-purification (step 3.2), and post purification (step 4.7), alongside a scaffold DNA sample and a 1 kb DNA marker, onto the gel. An example is given in **Figure 2**. Actual volumes of samples depend on the concentrations obtained after purification. Each samples is loaded with loading buffer at a 1:6 final volume ratio.
3. Set power source to 80 V and run gel for 3 hr. Run the gel in a bath filled with ice and water. Nanorobots will unfold and appear as a smear if the agarose gel heats up during electrophoresis. During electrophoresis add additional ice to keep device from heating.
4. View gel on a UV table (**Figure 2**).

6. Negative Stain of Nanorobot with Uranyl-formate

1. Preparation of 2% uranyl-formate stock solution (adapted from Castro et al.[23]):
    1. Weigh 100 mg of uranyl-formate powder into a 15 ml tube.
    2. Boil DNase/RNase free ultrapure water for 3 min to de-oxygenate.
    3. Add 5 ml of deoxygenated hot water (~60 °C) into the 15 ml tube containing the uranyl-formate powder (from previous step). Tightly close lid, wrap in aluminum foil and vortex rigorously for 10 min (fasten tube to a vortex). Solution should appear turbid with a yellow color.
    4. Filter solution through a 0.2 µm syringe filter. Solution should become clear.
    5. Aliquot 200 µl of the solution into microcentrifuge tubes.
    6. Centrifuge at max speed for 5 min in a table top centrifuge to pool samples at the bottom of the tube.

2. Loading of sample to grid and negative staining:
    1. Defrost a 200 µl aliquot of 2% uranyl-formate solution (prepared in section 6.1). Add 10 µl of 0.5 M NaOH solution and vortex rigorously for 3 min. Centrifuge at max speed for 5 minutes using a table top centrifuge.
    2. Meanwhile, glow-discharge grid using room air at 0.2 mbar and 25 mA for 30 sec.
    3. Add 15 µl of 2 nM nanorobot sample after purification (section 4.7) onto topside of grid (held with forceps) and let absorb for 1 min. Use filter paper to drain the excess liquid by placing the grid on top of the filter paper. Do not touch the grid surface.
    4. Add 10 µl of the 2% uranyl-formate (from step 6.2.1) onto the topside of grid (held with forceps).
    5. Quickly use filter paper to drain the excess liquid by placing the grid on top of the filter paper. Do not touch the grid surface.
    6. Repeat steps 6.2.4 and 6.2.5.
    7. Add 10 µl of the 2% uranyl-formate (from step 6.2.1) onto the topside of grid (held with forceps). Let staining solution absorb for 30 sec.
    8. Use filter paper to drain the excess liquid by placing the grid on top of the filter paper. Do not touch the grid surface.
    9. Let the grid dry completely for at least 30 min, face up on a filter paper, before injecting into the TEM.

Representative Results

Representative results are shown in **Figure 2A**. All lanes contain 1 µg of total DNA, measured via spectrophotometer (OD_{260}). Compared with the circular single-strand DNA scaffold (Lane 2), nanorobots are hindered in the gel due to their higher molecular weight, the result of staples hybridization to the scaffold DNA (Lane 3. Red arrow). The low molecular weight band in Lane 3 represents excess staples which did not bind to the scaffold DNA (Green arrow). After purification via centrifugal filtration most of the excess staples are removed (Lanes 4-6) and the nanorobots are ready to be loaded with cargo molecules conjugated to the Handles complementary strand[14,15,22]. Lanes 4-6 contain high molecular weight bands representing nanorobot dimers (Blue arrow), a population of nanorobots which are bound together. Reducing the concentration of the scaffold in the fabrication procedure (to either 5 or 10 nM) can potentially reduce the relative amount of these high molecular weight structures. Lanes 4-6 show nanorobots post-purification with slight variations to the described purification protocol, namely the initial volume of fabricated nanorobots added to the spin filter (Step 4.1. Lane 4: 50 µl; Lane 5: 100 µl; Lane 6: 100 µl), and the number of times the buffer was added to the filter (Step 4.4. Lane 4: 2 times; Lane 5: 2 times; Lane 6: 5 times).

Comparison of the yield and purification results between the different variations to the protocol (**Figure 2C**) show that reducing the initial volume of fabricated robots loaded unto the centrifugal filter (Step 4.1) has little effect on the yield and purification rates. Moreover, increasing the number of buffer exchanges and centrifugal spins (steps 4.4) has marginal influence on the purity on the nanorobots, while considerably reducing the yield. Hence the described protocol, corresponding to 100 µl initial volume and 2 buffer additions (Lane 5), is considered optimal.

Yield estimations are based on spectrophotometer (OD_{260}) measurements of each sample post-purification and calculated relative to the initial amount loaded into each centrifugal filter. Purification is based on the weight percent of the nanorobots from the entire DNA in the sample, corresponding to the nanorobots and excess staples which did not wash out during purification. Purification estimations are calculated from the

relative intensity of the nanorobots (red and blue arrows in **Figure 2A**) to that of the excess staples (green arrow in **Figure 2B**). The relative nanorobots/staples intensities were normalized with the pre-purified sample (Lane 3), in which the total DNA weight of the staples (green arrow) is ~4.5 times that of the unpurified nanorobots (red arrow), corresponding to the initial 10:1 scaffold to staples molar ratio in the fabrication protocol.

Final validation of structural integrity is achieved via transmission electron microscopy using 2% uranyl-formate as a negative stain. Photos are presented in **Figure 3**.
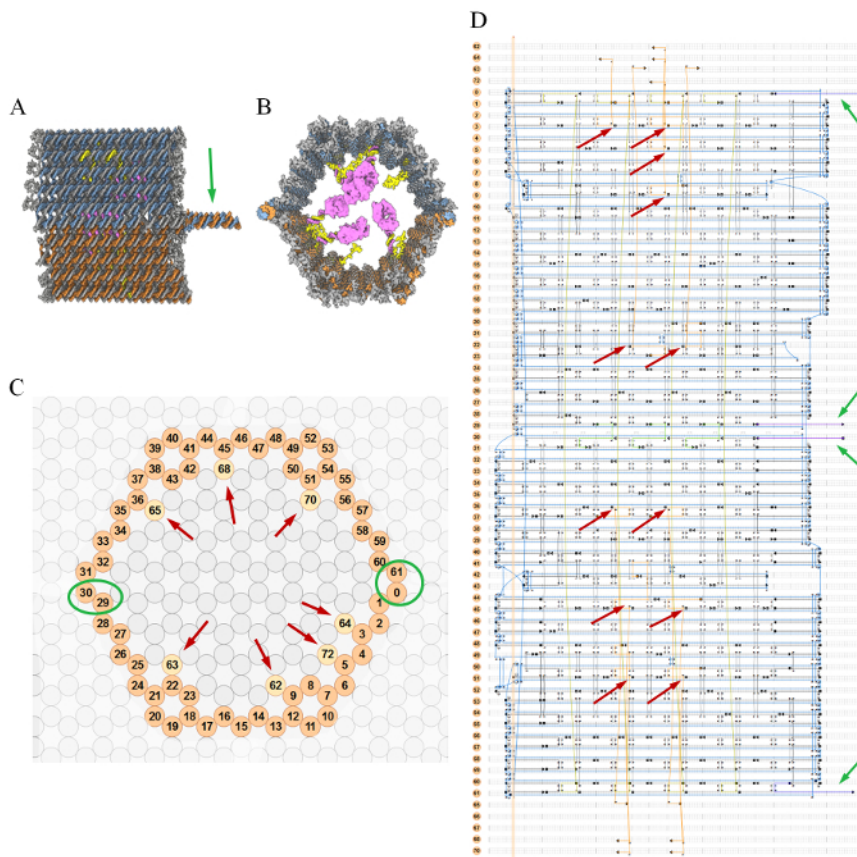

Figure 1: Design schematic of the nanorobot. (**A**) Side view of a closed nanorobot. Gate double helix, produced by an aptamer sequence and a complementary strand, is indicated by a green arrow. (**B**) Front view of a closed nanorobot showing protein cargo bound inside. (**C**) Cross-section schematics of closed nanorobot produced. Handles staples are highlighted by a red arrow. Green circles indicate helixes which contain a hinge on one side and a gate sequence at the opposite side. (**D**) Blueprints of a nanorobot at side view. Handles are indicated by red arrows. Gate sequences are indicated by green arrows. Please click here to view a larger version of this figure.
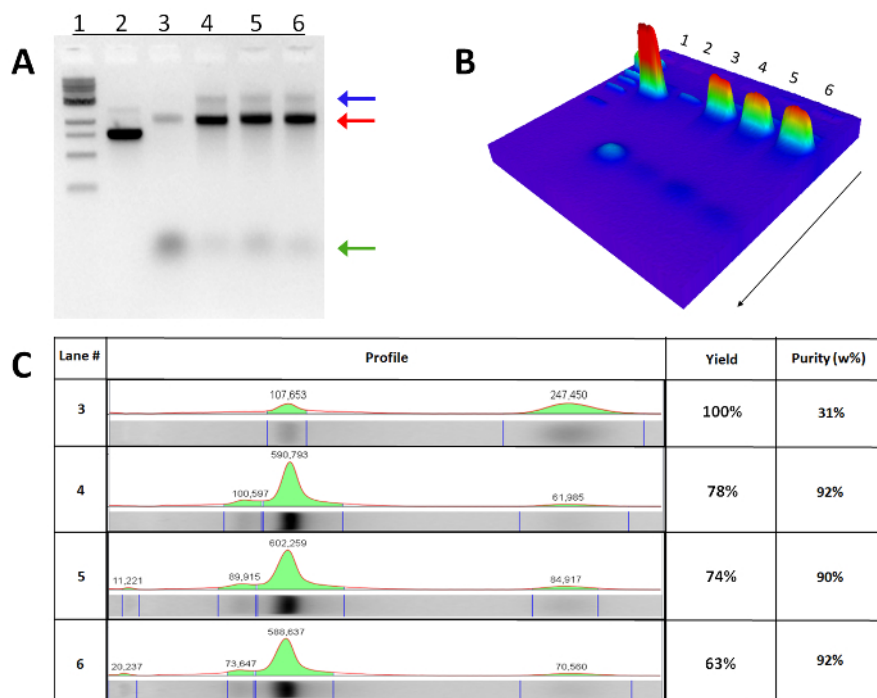
Figure 2: Agarose gel electrophoresis results. (**A**) Lane 1: 1kb Marker. Lane 2: M13mp18 circular single-strand scaffold. Lane 3: nanorobots pre-purification. Lanes 4-6: nanorobots post purifications. Lane 4: 50 μl initial volume; 2 buffer additions. Lane 5: 100 μl initial volume; 2 buffer additions. Lane 6: 100 μl initial volume; 5 buffer additions. Excess staples are indicated by a green arrow Fabricated nanorobots are indicated by a red arrow. Blue arrow indicated nanorobot dimers. (**B**) 3D view of the relative intensity of the bands in the agarose gel. (**C**) Yield and purification estimations.
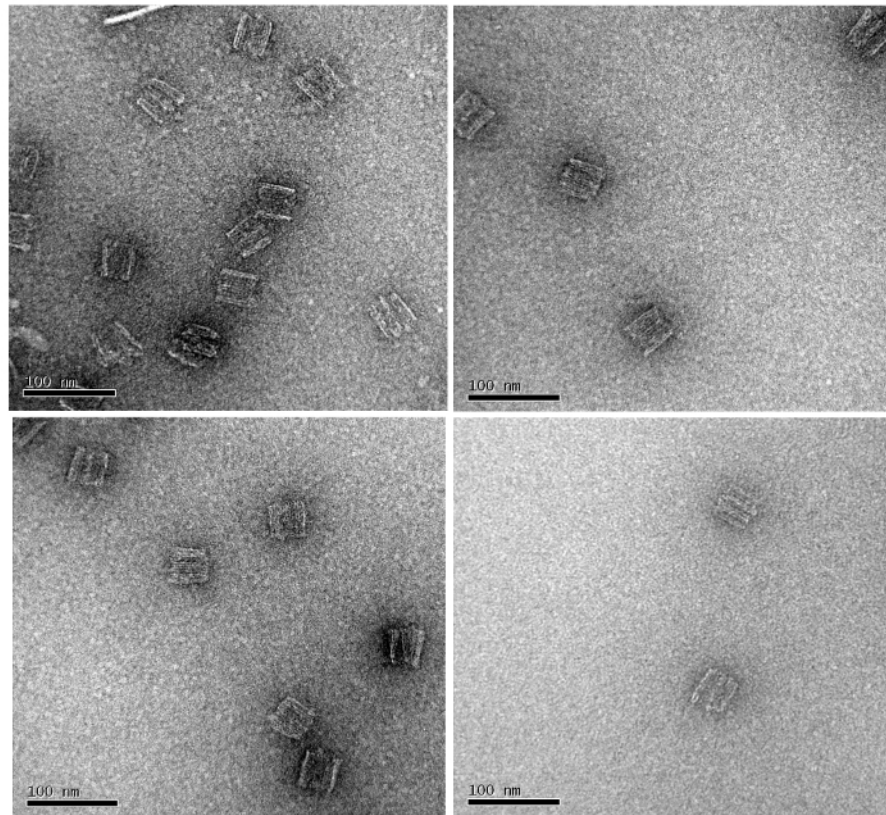

Figure 3: TEM photo of DNA nanorobots taken from multiple fabrications/staining procedures.

Number	Designation	Sequence
1	Core	AAAAACCAAACCCTCGTTGTGAATATGGTTTGGTC
2	Core	GGAAGAAGTGTAGCGGTCACGTTATAATCAGCAGACTGATAG
3	Core	TACGATATAGATAATCGAACAACA
4	Core	CTTTTGCTTAAGCAATAAAGCGAGTAGA
5	Core	GTCTGAAATAACATCGGTACGGCCGCGCACGG
6	Core	GGAAGAGCCAAACAGCTTGCAGGGAACCTAA
7	Core	AAAATCACCGGAAGCAAACTCTGTAGCT
8	Core	CCTACATGAAGAACTAAAGGGCAGGGCGGAGCCCCGGGC
9	Core	CATGTAAAAAGGTAAAGTAATAAGAACG
10	Core	ATTAAATCAGGTCATTGCCTGTCTAGCTGATAAATTGTAATA
11	Core	ATAGTCGTCTTTTGCGGTAATGCC
12	Core	AGTCATGGTCATAGCTGAACTCACTGCCAGT
13	Core	AACTATTGACGGAAATTTGAGGGAATATAAA
14	Core	ATCGCGTCTGGAAGTTTCATTCCATATAGAAAGACCATC
15	Core	AAATATTGAACGGTAATCGTAGCCGGAGACAGTCATAAAAAT
16	Core	GTCTTTACAGGATTAGTATTCTAACGAGCATAGAACGC
17	Core	GCACCGCGACGACGCTAATGAACAGCTG
18	Core	AACTTCATTTTAGAATCGCAAATC
19	Core	CGTAGAGTCTTTGTTAAGGCCTTCGTTTTCCTACCGAG
20	Core	CCAATCAAAGGCTTATCCGGTTGCTATT
21	Core	AGAGGCGATATAATCCTGATTCATCATA
22	Core	CCGTAATCCCTGAATAATAACGGAATACTACG
23	Core	AAATGGTATACAGGGCAAGGAAATC
24	Core	TCCTCATCGTAACCAAGACCGACA
25	Core	CATTATCTGGCTTTAGGGAATTATGTTTGGATTAC
26	Core	ACCCGCCCAATCATTCCTCTGTCC
27	Core	CGACCAGTCACGCAGCCACCGCTGGCAAAGCGAAAGAAC
28	Core	CTAAAGGCGTACTATGGTTGCAACAGGAGAGA
29	Core	TTGGCAGGCAATACAGTGTTTCTGCGCGGGCG
30	Core	TATACAGGAAATAAAGAAATTTTGCCCGAACGTTAAGACTTT
31	Core	AAGTATAGTATAAACAGTTAACTGAATTTACCGTTGAGCCAC
32	Core	ACATTCAGATAGCGTCCAATATTCAGAA
33	Core	AAACATCTTTACCCTCACCAGTAAAGTGCCCGCCC
34	Core	GAGATGACCCTAATGCCAGGCTATTTTT
35	Core	TCCTGAATTTTTTGTTTAACGATCAGAGCGGA
36	Core	GCCGAAAAATCTAAAGCCAATCAAGGAAATA
37	Core	AGCGTAGCGCGTTTTCACAAAATCTATGTTAGCAAACGAACGCAACAAA
38	Core	ACCAATCGATTAAATTGCGCCATTATTA
39	Core	ATCTTACTTATTTTCAGCGCCGACAGGATTCA
40	Core	CCCTAAAAGAACCCAGTCACA
41	Core	GGAAGGGCGAAAATCGGGTTTTTCGCGTTGCTCGT
42	Core	CAGACCGGAAGCCGCCATTTTGATGGGGTCAGTAC
43	Core	TAATATTGGAGCAAACAAGAGATCAATATGATATTGCCTTTA
44	Core	TTCCTTATAGCAAGCAAATCAAATTTTA

45	Core	ACTACGAGGAGAGATTTTTTCACGTTGAAACTTGCTTT
46	Core	AAACAGGCATGTCAATCATATAGATTCAAAAGGGTTATATTT
47	Core	AACAGGCACCAGTTAAAGGCCGCTTTGTGAATTTCTTA
48	Core	TTCCTGAGTTATCTAAAATATTCAGTTGTTCAAATAGCAG
49	Core	AAAGAAACAAGAGAAGATCCGGCT
50	Core	TTGAGGGTTCTGGTCAGGCTGTATAAGC
51	Core	TTTAACCGTCAATAGTGAATTCAAAAGAAGATGATATCGCGC
52	Core	ACGAGCGCCCAATCCAAATAAAATTGAGCACC
53	Core	AATAAGTCGAAGCCCAATAATTATTTATTCTT
54	Core	ACGAAATATCATAGATTAAGAAACAATGGAACTGA
55	Core	TTTCATAGTTGTACCGTAACACTGGGGTTTT
56	Core	AGGAGCGAGCACTAACAACTAAAACCCTATCACCTAACAGTG
57	Core	CAAAGTATTAATTAGCGAGTTTCGCCACAGAACGA
58	Core	TGGGGAGCTATTTGACGACTAAATACCATCAGTTT
59	Core	ATAACGCAATAGTAAAATGTTTAAATCA
60	Core	ACGAATCAACCTTCATCTTATACCGAGG
61	Core	TAATGGTTTGAAATACGCCAA
62	Core	CGGAACAAGAGCCGTCAATAGGCACAGACAATATCCTCAATC
63	Core	ATTAAAGGTGAATTATCAAAGGGCACCACGG
64	Core	GGCAACCCATAGCGTAAGCAGCGACCATTAA
65	Core	AGAAACGTAAGCAGCCACAAGGAAACGATCTT
66	Core	AGAGGTCTTTAGGGGGTCAAAAGGCAGT
67	Core	GGGGACTTTTTCATGAGGACCTGCGAGAATAGAAAGGAGGAT
68	Core	TTTTAGAACATCCAATAAATCCAATAAC
69	Core	AAATGTGGTAGATGGCCCGCTTGGGCGC
70	Core	ACGGATCGTCACCCTCACGATCTAGAATTTT
71	Core	CGCCATAAGACGACGACAATAGCTGTCT
72	Core	GCGTATTAGTCTTTAATCGTAAGAATTTACA
73	Core	AGAGAACGTGAATCAAATGCGTATTTCCAGTCCCC
74	Core	AACGAAAAAGCGCGAAAAAAAGGCTCCAAAAGG
75	Core	TAATTTAGAACGCGAGGCGTTAAGCCTT
76	Core	ACCAGGCGTGCATCATTAATTTTTTCAC
77	Core	CAGCCTGACGACAGATGTCGCCTGAAAT
78	Core	ATTAGTCAGATTGCAAAGTAAGAGTTAAGAAGAGT
79	Core	CTCGAATGCTCACTGGCGCAT
80	Core	GGGCAGTCACGACGTTGAATAATTAACAACC
81	Core	TAAAAACAGGGGTTTTGTTAGCGAATAATATAATAGAT
82	Core	TCAACCCTCAGCGCCGAATATATTAAGAATA
83	Core	ATTATACGTGATAATACACATTATCATATCAGAGA
84	Core	GCAAATCTGCAACAGGAAAAATTGC
85	Core	ATAATTACTAGAAATTCTTAC
86	Core	TATCACCGTGCCTTGAGTAACGCGTCATACATGGCCCCTCAG
87	Core	AAGTAGGGTTAACGCGCTGCCAGCTGCA
88	Core	CCAGTAGTTAAGCCCTTTTTAAGAAAAGCAAA
89	Core	TGGCGAAGTTGGGACTTTCCG
90	Core	CAGTGAGTGATGGTGGTTCCGAAAACCGTCTATCACGATTTA

91	Core	AAATCAAAGAGAATAACATAACTGAACACAGT
92	Core	CTGTATGACAACTAGTGTCGA
93	Core	ATCATAAATAGCGAGAGGCTTAGCAAAGCGGATTGTTCAAAT
94	Core	TTGAGTAATTTGAGGATTTAGCTGAAAGGCGCGAAAGATAAA
95	Core	ATAAGAATAAACACCGCTCAA
96	Core	CGTTGTAATTCACCTTCTGACAAGTATTTTAA
97	Core	AACCGCCTCATAATTCGGCATAGCAGCA
98	Core	AAATAGGTCACGTTGGTAGCGAGTCGCGTCTAATTCGC
99	Core	CAGTATAGCCTGTTTATCAACCCCATCC
100	Core	TTGCACCTGAAAATAGCAGCCAGAGGGTCATCGATTTTCGGT
101	Core	CGTCGGAAATGGGACCTGTCGGGGGAGA
102	Core	AAGAAACTAGAAGATTGCGCAACTAGGG
103	Core	CCAGAACCTGGCTCATTATACAATTACG
104	Core	ACGGGTAATAAATTAAGGAATTGCGAATAGTA
105	Core	CCACGCTGGCCGATTCAAACTATCGGCCCGCT
106	Core	GCCTTCACCGAAAGCCTCCGCTCACGCCAGC
107	Core	CAGCATTAAAGACAACCGTCAAAAATCA
108	Core	ACATCGGAAATTATTTGCACGTAAAAGT
109	Core	CAACGGTCGCTGAGGCTTGATACCTATCGGTTTATCAGATCT
110	Core	AAATCGTACAGTACATAAATCAGATGAA
111	Core	TTAACACACAGGAACACTTGCCTGAGTATTTG
112	Core	AGGCATAAGAAGTTTTGCCAGACCCTGA
113	Core	GACGACATTCACCAGAGATTAAAGCCTATTAACCA
114	Core	AGCTGCTCGTTAATAAAACGAGAATACC
115	Core	CTTAGAGTACCTTTTAAACAGCTGCGGAGATTTAGACTA
116	Core	CACCCTCTAATTAGCGTTTGCTACATAC
117	Core	GAACCGAAAATTGGGCTTGAGTACCTTATGCGATTCAACACT
118	Core	GCAAGGCAGATAACATAGCCGAACAAAGTGGCAACGGGA
119	Core	ATGAAACAATTGAGAAGGAAACCGAGGATAGA
120	Core	GGATGTGAAATTGTTATGGGGTGCACAGTAT
121	Core	GGCTTGCGACGTTGGGAAGAACAGATAC
122	Core	TAAATGCCTACTAATAGTAGTTTTCATT
123	Core	TGCCGTCTGCCTATTTCGGAACCAGAATGGAAAGCCCACCAGAAC
124	Core	TGACCATAGCAAAAGGGAGAACAAC
125	Core	CGAGCCAGACGTTAATAATTTGTATCA
126	Core	GCTCAGTTTCTGAAACATGAAACAAATAAATCCTCCCGCCGC
127	Core	AGACGCTACATCAAGAAAACACTTTGAA
128	Core	AGTACTGACCAATCCGCGAAGTTTAAGACAG
129	Core	GATTCCTGTTACGGGCAGTGAGCTTTTCCTGTGTGCTG
130	Core	GGTATTAAGGAATCATTACCGAACGCTA
131	Core	GTTCATCAAATAAAACGCGACTCTAGAGGATCGGG
132	Core	AGCCTTTAATTGGATAGTTGAACCGCCACCCTCATAGGTG
133	Core	ACAGAGGCCTGAGATTCTTTGATTAGTAATGG
134	Core	AACGAGATCAGGATTAGAGAGCTTAATT
135	Core	TACCAAGTTATACTTCTGAATCACCAGA
136	Core	CAGTAGGTGTTCAGCTAATGCGTAGAAA

137	Core	AGGATGACCATAGACTGACTAATGAAATCTACATTCAGCAGGCGCGTAC
138	Core	TTTCAACCAAGGCAAAGAATTTAGATAC
139	Core	TTGAAATTAAGATAGCTTAACTAT
140	Core	CTATTATCGAGCTTCAAAGCGTATGCAA
141	Core	CAGGGTGCAAAATCCCTTATAGACTCCAACGTCAAAAGCCGG
142	Core	GAGCTTGTTAATGCGCCGCTAATTTTAGCGCCTGCTGCTGAA
143	Core	CGAACGTTAACCACCACACCCCCAGAATTGAG
144	Core	GTGTGATAAATAAGTGAGAAT
145	Core	GCTATATAGCATTAACCCTCAGAGA
146	Core	AGGAGAGCCGGCAGTCTTGCCCCCGAGAGGGAGGG
147	Core	CGGCCTCCAGCCAGAGGGCGAGCCCCAA
148	Core	CCAAAACAAAATAGGCTGGCTGACGTAACAA
149	Core	GGCGGTTAGAATAGCCCGAGAAGTCCACTATTAAAAAGGAAG
150	Core	ATAAAGGTTACCAGCGCTAATTCAAAAACAGC
151	Core	ATTGCCCCCAGCAGGCGAAAAGGCCCACTACGTGACGGAACC
152	Core	TTTTAAAACATAACAGTAATGGAACGCTATTAGAACGC
153	Core	AATTGGGTAACGCCAGGCTGTAGCCAGCTAGTAAACGT
154	Edge	TTACCCAGAACAACATTATTACAGGTTTTTTTTTTTTTTTT
155	Edge	TTTTTTTTTTTTTTTTAATAAGAGAATA
156	Edge	TTTTTTTTTTTTTTTTCCAGTTTGGGAGCGGGCTTTTTTTTTTTTTTTT
157	Edge	GGTTGAGGCAGGTCAGTTTTTTTTTTTTTTTT
158	Edge	TTTTTTTTTTTTTTTTGATTAAGACTCCTTATCCAAAAGGAAT
159	Edge	TTTTTTTTTTTTTTTTCTTCGCTATTACAATT
160	Edge	TTTTTTTTTTTTTTTTCTTGCGGGAGAAGCGCATTTTTTTTTTTTTTTT
161	Edge	TTTTTTTTTTTTTTTGGGAATTAGAGAAACAATGAATTTTTTTTTTTTTTTT
162	Edge	TCAGACTGACAGAATCAAGTTTGTTTTTTTTTTTTTTTT
163	Edge	TTTTTTTTTTTTTTTTGGTCGAGGTGCCGTAAAGCAGCACGT
164	Edge	TTTTTTTTTTTTTTTTTTAATCATTTACCAGACTTTTTTTTTTTTTTTT
165	Edge	TTTTTTTTTTTTTCATTCTGGCCAAATTCGACAACTCTTTTTTTTTTTTTT
166	Edge	TTTTTTTTTTTTTTTACCGGATATTCA
167	Edge	TTTTTTTTTTTTTTTTAGACGGGAAACTGGCATTTTTTTTTTTTTTTT
168	Edge	TTTTTTTTTTTTTTTTCAGCAAGCGGTCCACGCTGCCCAAAT
169	Edge	CTGAGAGAGTTGTTTTTTTTTTTTTTTT
170	Edge	CAATGACAACAACCATTTTTTTTTTTTTTTTT
171	Edge	TTTTTTTTTTTTTTTTGAGAGATCTACAAGGAGAGG
172	Edge	TCACCAGTACAAACTATTTTTTTTTTTTTTTT
173	Edge	TTTTTTTTTTTTTGGCAATTCATCAAATTATTCATTTTTTTTTTTTTTTTT
174	Edge	TAAAGTTACCGCACTCATCGAGAACTTTTTTTTTTTTTTTT
175	Edge	TTTTTTTTTTTTTTTTCACCCTCAGAACCGCC
176	Edge	TTTTTTTTTTTTTAGGTTTAACGTCAATATATGTGAGTTTTTTTTTTTTTT
177	Edge	CCACACAACATACGTTTTTTTTTTTTTT
178	Edge	TTTTTTTTTTTTTTTTGCTAGGGCGAGTAAAAGATTTTTTTTTTTTTTTT
179	Edge	TTTTTTTTTTTTTTTTTAGTTGATTCCCAATTCTGCGAACCTCA
180	Edge	TTATTTAGAGCCTAATTTGCCAGTTTTTTTTTTTTTTTTTT
181	Edge	TTTTTTTTTTTTTTTTACGGCGGAT
182	Edge	TTTTTTTTTTTTTTTTATATGCGTTAAGTCCTGATTTTTTTTTTTTTTTT

December 2015 | 106 | e51272 | Page 9 of 13

183	Edge	TTTTTTTTTTTTTTTTACGATTGGCCTTGATA
184	Edge	TTTTTTTTTTTTTTTTCAACGCCTGTAGCATT
185	Edge	TTTTTTTTTTTTTTTTGGCTTTGAGCCGGAACGATTTTTTTTTTTTTTT
186	Edge	TTTTTTTTTTTTTTTTAAGCAAGCCGTTT
187	Edge	TTTTTTTTTTTTTTTTATGTGTAGGTAAGTACCCCGGTTGTTTTTTTTTTTTTT
188	Edge	ATCGTCATAAATATTCATTTTTTTTTTTTTTTTTT
189	Edge	TTTTTTTTTTTTTTTTGTTAATTTCATCT
190	Edge	TTTTTTTTTTTTTTTTGTATTAAATCCTGCGTAGATTTTCTTTTTTTTTTTTTT
191	Edge	GCCATATAAGAGCAAGCCAGCCCGACTTGAGCCATGGTT
192	Edge	GTAGCTAGTACCAAAAACATTCATAAAGCTAAATCGGTTTTTTTTTTTTTT
193	Edge	ATAACGTGCTTTTTTTTTTTTTTTTTTTT
194	Edge	TTTTTTTTTTTTTTTTAAAAATACCGAACGAACCACCAGTGAGAATTAAC
195	Edge	TTTTTTTTTTTTTTTTACAAAATAAACA
196	Edge	TTTTTTTTTTTTTTTTACAAGAAAAACCTCCCGATTTTTTTTTTTTTTT
197	Edge	TTTTTTTTTTTTTTTTGACGATAAAAAGATTAAGTTTTTTTTTTTTTTTT
198	Edge	TTTTTTTTTTTTTTCAATTACCTGAGTATCAAAATCATTTTTTTTTTTTTTT
199	Edge	GGTACGGCCAGTGCCAAGCTTTTTTTTTTTTTTTT
200	Edge	TTTTTTTTTTTTTTTTGAATAACCTTGAAATATATTTTATTTTTTTTTTTTTT
201	Edge	CACTAAAACACTTTTTTTTTTTTTTTTTT
202	Edge	TTTTTTTTTTTTTTTTTTAACCAATATGGGAACAATTTTTTTTTTTTTTTT
203	Edge	TACGTCACAATCAATAGAATTTTTTTTTTTTTTTTT
204	Edge	TTTTTTTTTTTTTTTTAGAAAGATTCATCAGTTGA
205	Edge	TTTTTTTTTTTTTTGTGGCATCAATTAATGCCTGAGTATTTTTTTTTTTTTT
206	Edge	TTTTTTTTTTTTTTTTTTGCATGCCTGCATTAATTTTTTTTTTTTTTTTT
207	Edge	CCAGCGAAAGAGTAATCTTGACAAGATTTTTTTTTTTTTTT
208	Edge	TTTTTTTTTTTTTTTTGAATCCCCCTCAAATGCTT
209	Edge	AGAGGCTGAGACTCCTTTTTTTTTTTTTTTTT
210	Edge	ACAAACACAGAGATACATCGCCATTATTTTTTTTTTTTTTTT
211	Edge	TTTTTTTTTTTTTTTTCAAGAGAAGGATTAGG
212	Edge	TTTTTTTTTTTTTTTGAATTGAGGAAGTTATCAGATGATTTTTTTTTTTTTT
213	Edge	CAGAACAATATTTTTTTTTTTTTTTTTT
214	Edge	TTTTTTTTTTTTTTAGCCGGAAGCATAAAGTGTCCTGGCC
215	Edge	TGACCGTTTCTCCGGGAACGCAAATCAGCTCATTTTTTTTTTTTTTTTTTTT
216	Edge	TTTTTTTTTTTTTTTTGGTAATAAGTTTTAAC
217	Edge	TTTTTTTTTTTTTTTGTCTGTCCATAATAAAAGGGATTTTTTTTTTTTTTT
218	Edge	TTTTTTTTTTTTTTTTTCCTCGTTAGAATCAGAGCGTAATATC
219	Edge	AATTGCTCCTTTTGATAAGTTTTTTTTTTTTTTT
220	Edge	CATCGGACAGCCCTGCTAAACAACTTTCAACAGTTTTTTTTTTTTTTTTT
221	Edge	TTTTTTTTTTTTTTTTTAACCGCCTCCCTCAGACCAGAGC
222	Edge	TCTGACAGAGGCATTTTCGAGCCAGTTTTTTTTTTTTTTTT
223	Edge	TTTTTTTTTTTTTTTTTTTCAGCGGAGTTCCATGTCATAAGG
224	Edge	TTTTTTTTTTTTTTTTCGCCCACGCATAACCG
225	Edge	AATTACTTAGGACTAAATAGCAACGGCTACAGATTTTTTTTTTTTTTTT
226	Edge	CAAGTTTTTTGGTTTTTTTTTTTTTTTTT
227	Edge	TTTTTTTTTTTTTTTTCCTTTAGCGCACCACCGGTTTTTTTTTTTTTTTT
228	Edge	TTTTTTTTTTTTTTTTTGAATCGGCCGAGTGTTGTTTTTTTTTTTTTTTT

229	Edge		TTTTTTTTTTTTTCATCTTTGACCC
230	Edge		TTTTTTTTTTTTTATAATCAGAAAATCGGTGCGGGCCTTTTTTTTTTTTTT
231	Edge		GATACAGGAGTGTACTTTTTTTTTTTTTTTT
232	Edge		TTTTTTTTTTTTTTGGCGCAGACAATTTCAACTTTTTTTTTTTTTTT
233	Edge		GGAGGTTTAGTACCGCTTTTTTTTTTTTTTTT
234	Edge		TTTTTTTTTTTTTACCGCCAGCCATAACAGTTGAAAGTTTTTTTTTTTTT
235	Edge		TTTTTTTTTTTTTTTATAGCAATAGCT
236	Handles		AATAAGTTTTGCAAGCCCAATAGGGGATAAGTTGTGCTACTCCAGTTC
237	Handles		ACATAGCTTACATTTAACAATAATAACGTTGTGCTACTCCAGTTC
238	Handles		CCTTTTTGAATGGCGTCAGTATTGTGCTACTCCAGTTC
239	Handles		CGTAACCAATTCATCAACATTTTGTGCTACTCCAGTTC
240	Handles		CACCAACCGATATTCATTACCATTATTGTGCTACTCCAGTTC
241	Handles		CCACCCTCATTTTCTTGATATTTGTGCTACTCCAGTTC
242	Handles		AACTTTGAAAGAGGAGAAACATTGTGCTACTCCAGTTC
243	Handles		CAAGGCGCGCCATTGCCGGAATTGTGCTACTCCAGTTC
244	Handles		CATAGCCCCCTTAAGTCACCATTGTGCTACTCCAGTTC
245	Handles		TTTCCCTGAATTACCTTTTTTACCTTTTTTGTGCTACTCCAGTTC
246	Handles		AACGGTGTACAGACTGAATAATTGTGCTACTCCAGTTC
247	Handles		GATTCGCGGGTTAGAACCTACCATTTTGTTGTGCTACTCCAGTTC
248	Guides		AGAGTAGGATTTCGCCAACATGTTTTAAAAACC
249	Guides		ACGGTGACCTGTTTAGCTGAATATAATGCCAAC
250	Guides		CGTAGCAATTTAGTTCTAAAGTACGGTGTTTTA
251	Guides		GCTTAATGCGTTAAATGTAAATGCTGATCTTGAAATGAGCGTT
252	Guides		AAGCCAACGGAATCTAGGTTGGGTTATATAGATTAAGCAACTG
253	Guides		TTTAACAACCGACCCAATCGCAAGACAAAATTAATCTCACTGC
254	Guides		TTTAGGCCTAAATTGAGAAAACTTTTTCCTTCTGTTCCTAGAT
255	Guides Removal		GGTTTTTAAAACATGTTGGCGAAATCCTACTCT
256	Guides Removal		GTTGGCATTATATTCAGCTAAACAGGTCACCGT
257	Guides Removal		TAAAACACCGTACTTTAGAACTAAATTGCTACG
258	Guides Removal		AACGCTCATTTCAAGATCAGCATTTACATTTAACGCATTAAGC
259	Guides Removal		CAGTTGCTTAATCTATATAACCCAACCTAGATTCCGTTGGCTT
260	Guides Removal		GCAGTGAGATTAATTTTGTCTTGCGATTGGGTCGGTTGTTAAA
261	Guides Removal		ATCTAGGAACAGAAGGAAAAAGTTTTCTCAATTTAGGCCTAAA
262	Gates	Gate29	TGGGGCGCGAGCTGAAAAGTACTCAGGGCACTGCAAGCAATTGTGGTCCCAATGGGCTGAGTA
263	Gates	Gate30	TACTCAGCCCATTGGGTTTTTTTTTTTTTTTTTTTTTTTTTTTTTTAGGTCTGAGAGACTACCTT
264	Gates	Gate0	TGATGAGCGTGGATGATACTCAGCCCATTGGGTTTTTTTTTTTTTTTTTTTTTTTTTTTTTTAGGTCATTTTTGCG-GATGG
265	Gates	Gate61	ATACAAAAAGCCTGTTTAGTATCTACTCAGGGCACTGCAAGCAATTGTGGTCCCAATGGGCTGAGTA

Table 1: List of staple sequences used to construct the nanorobot. Staples 1-153 are designated Core and make up the bulk of the structure. Staples 154-235 are designated Edges and are situated at each of the ends of the 61 helixes of the structure. Edge staples contain a poly thymine tail designed to avoid aggregation of nanorobots. Staples 236-247 are designated Handles and make up the cargo docking sites. Handles staples have a unique sequence region, connecting them to their specific location of the structure, and a consensus sequence region which is used as docking site for the cargo molecules. Staples 248-254 are designated Guides and attach the two halves of the device during the annealing process. After fabrication the Guides are removed with the addition of Guide Removal staples 255-261 (step 6), leaving the device locked by the two sensors of the nanorobot. Sensor sequences are designated Gates. Each of the two sensors is made up of a PDGF aptamer and a complementary strand. For a more detailed explanation see Ben-Ishay *et al.*[14] and Douglas *et al.*[15]. Staples are ordered commercially on three 96-well plates (deep round bottom). Each staple amount is normalized to 10 nmol. Except for the Gate sequences, which require HPLC purification, staples do not require a special purification procedure.

Discussion

We described the fabrication, purification, and visualization of the DNA nanorobot. Following fabrication of the hexagonal chassis of the device, the function of the nanorobot is programmed with the simple introduction of specific cargo and sensing strands to the robot which readily find their designated position due to hydrogen-bonding complementarity with available single-strand docking sites[14,15,22].

The fabrication protocol described uses a slow annealing ramp, which is generally used in our lab to fold a wide range of origami shapes. If production time becomes a key factor other protocols, such as the rapid folding protocol described by Sobczak *et al.*[24] can be used. This protocol is reported to achieve origami folding in high yields, however it requires calibration for each origami shape.

Spin filtration is used to purify the robots from excess staples. When loading the spin column with samples or buffer, care should be taken not to damage the membrane with the pipette tip. The membrane can potentially rupture resulting in dramatically reduced yields. It is advisable to not discard the flow-through until the nanorobots are visualized by AGE.

For certain application a higher purification rate is desired; this can be achieved by repeating the filtration using the original spin column. For even higher purity, a new spin column can be used, however this will have a dramatic negative effect on the yield rates. Other methods for purifying DNA origami structures were tested, such as excision from agarose gel subsequent to electrophoresis and dialysis of excess staples. These methods resulted in either poor yield or poor purification rates compared with the described protocol. Other methods, such as PEG-based purification[25] and rate-zonal ultracentrifugation[26] were not tested. These methods are reported to achieve high purification rates, however they either result in poor yields (rate-zonal ultracentrifugation) or require precipitation (PEG-based) which can potentially harm the hollow nanorobot shape.

Nanorobots are fabricated with Guide staples which lock the shape in the closed position in order to increase fabrication yeilds[15]. It is important to remove these staples by adding Guide Removal staples for nanorobots to effectively open in response to the designed stimuli (PDGF in the described protocol). Guide staples are designed with a toehold single strand region for the docking of Guide Removal staples which release the Guide staples through a process of strand displacement[18].These staples should be added at a 10:1 molar ratio at the end of the purification of excess staples' stage (step 4.7) and incubated for 2 hr at room temperature on an end over end shaker.

Visualization by TEM was described, including uranyl-formate 2% negative staining. Compared with uranyl-acetate, uranyl-formate produces finer grain structures which allow for better resolution of DNA origami designs. Care should be taken as uranyl-formate will solidify if aliquots are frozen for long periods of time. It is advisable to use a freshly prepared 2% uranyl-formate solution for staining. Better resolutions are achievable with the use of Cryo-TEM[27].

The basic architectural design and fabrication protocol of the DNA nanorobot are ultimately uniform and straightforward. However, a wide range of flexibility is offered in the form of specific cargo mixtures and sensing strands. Moreover, in a single population many subtypes can be introduced and their relative stoichiometry programmed and optimized to fit specific needs. Even greater fine tuning of the specific kinetics at each rate-limiting step is achievable with increasing/reducing the length of double strand hybridization or the introduction of mismatches at specific key positions. This high degree of flexibility with ease of construction allows for the engineering of nanoscale devices capable of performing highly varied complex tasks in a biological relevant milieu.

Disclosures

The authors have nothing to disclose.

Acknowledgements

References

1. Watson, J. D., & Crick, F. H. Genetical implications of the structure of deoxyribonucleic acid. *Nature.* **171**, 964-967 (1953).
2. Kosuri, S., & Church, G. M. Large-Scale *de novo*. DNA synthesis: technologies and applications. *Nature Meth.* **11** (5), 499-507 (2014).
3. Pinheiro A. V., Han D., Shih, W. M., Yan, H. Challenges and opportunities for structural DNA nanotechnology. *Nature Nanotech.* **6** (12), 763-772 (2011).
4. Seeman, N. C. Nucleic acid junctions and lattices. *J Theor Biol.* **99** (2), 237-247 (1982).
5. Chen, J. H., & Seeman, N. C. Synthesis from DNA of a molecule with the connectivity of a cube. *Nature.* **350** (6319), 631-633 (1991).
6. Wei, B., Dai, M., & Yin, P. Complex shapes self-assembled from single-stranded DNA tiles. *Nature.* **485** (7400), 623-626 (2012).
7. He, Y. *et al.* Hierarchical self-assembly of DNA into symmetric supramolecular polyhedra. *Nature.* **452** (7184), 198-201 (2008).
8. Yin, P., Hariadi, R. F., Sahu, S., Choi, H. M. T., Park, S. H., Labean, T. H., Reif, J. H. Programming DNA tube circumferences. *Science.* **321** (5890), 824-826 (2008).
9. Rothemund, P. W. Folding DNA to create nanoscale shapes and patterns. *Nature.* **440** (7082) 297-302, (2006).
10. Dietz, H., Douglas, S. M., & Shih, W. M. Folding DNA into twisted and curved nanoscale shapes. *Science.* **325** (5941), 725-730 (2009).
11. Douglas, S. M., *et al.Self-assembly of DNA into nanoscale three-dimensional shapes.Nature.* **459** (7245), 414-418 (2009).

12. Zhang, F., Nangreave, J., Liu, Y., Yan, H. Structural DNA nanotechnology: state of the art and future perspective. *J Am Chem Soc.* **136** (32) 11198-11211, (2014).
13. Douglas, S. M., *et al*.prototyping of 3D DNA-origami shapes with caDNAno*. Nucleic Acids Res.* **37** (15), 5001-5006 (2009).
14. Ben-Ishay, E., Abu-Horowitz, A., Bachelet, I. Designing a bio-responsive robot from DNA origami. *J Vis Exp.* (77), e50268 (2013).
15. Douglas, S. M., Bachelet, I., & Church, G. M. A logic-gated nanorobot for targeted transport of molecular payloads. *Science.* **335** (6070), 831-834 (2012).
16. Tan, W., Donovan, M. J., Jiang, J. Aptamers from cell-based selection for bioanalytical applications. *Chem Rev.* **113** (4), 2842-2862 (2013).
17. Xiang, D. *et al.* Nucleic Acid Aptamer-Guided Cancer Therapeutics and Diagnostics: The Next Generation of Cancer Medicine. *Theranostics.* **5** (1), 23-42 (2015).
18. Zhang, D. Y., & Seelig, G. Dynamic DNA nanotechnology using strand-displacement reactions. *Nat Chem.* **3** (2), 103-113 (2011).
19. Tang, Z., Parekh, P., Turner, P., Moyer, R. W., & Tan, W. Generating aptamers for recognition of virus-infected cells. *Clin Chem.* **55** (4), 813-822 (2009).
20. Sefah, K., Shangguan, D., Xiong, X., O'Donoghue M. B., Tan, W. Development of DNA aptamers using Cell-SELEX. *Nature Prot.* **5** (6), 1169-1185 (2010).
21. McKeague, M., & DeRosa, M. C. Challenges and Opportunities for Small Molecule Aptamer Development. *J Nucleic Acids.* **2012** (2012).
22. Amir, Y. *et al.* Universal computing by DNA origami robots in a living animal. *Nature Nanotech.* **9** (5), 353-357 (2014).
23. Castro, C. E., *et al*. A primer to scaffolded DNA origami. *Nature Meth.* **8** (3), 221-229 (2011).
24. Sobczak, J. P., Martin, T. G., Gerling, T., Dietz, H. Rapid folding of DNA into nanoscale shapes at constant temperature. *Science.* **338** (6113), 1458-1461 (2012).
25. Stahl, E., Martin, T. G., Praetorius, F., Dietz, H. Facile and scalable preparation of pure and dense DNA origami solutions. *Angew Chem Int Ed Engl.* **53** (47), 12735-12740 (2014).
26. Lin, C., Perrault, S. D., Kwak, M., Graf, F., Shih, W. M. Purification of DNA-origami nanostructures by rate-zonal centrifugation. *Nucleic Acids Res.* **41** (2), e40 (2012).
27. Bai, X. C., Martin, T. G., Scheres, S. H., Dietz, H. Cryo-EM structure of a 3D DNA-origami object. *Proc Natl Acad Sci U S A*. **109** (49), 20012-20017 (2012).